Asian Journal of Chemistry; Vol. 30, No. 8 (2018), 1787-1790

ASIAN JOURNAL OF CHEMISTRY

https://doi.org/10.14233/ajchem.2018.21306

Preparation and Characterization of Indonesian Natural Zeolite-Supported PbO Photocatalyst

M.P. UTOMO*, ATHOOURROHMAN, L.P. SARI and A.K. PRODJOSANTOSO

Department of Chemistry, Yogyakarta State University, Yogyakarta DIY 55281 Indonesia

*Corresponding author: E-mail: pranjoto_utomo@uny.ac.id

Received: 26 February 2018; *Accepted*: 15 May 2018; *Published online*: 30 June 2018; AJC-18975

Indonesian natural zeolite-supported PbO has been prepared and characterized. The zeolite-supported PbO was prepared by sol-gel method using natural zeolite and $Pb(CH_3COO)_2{\cdot}3H_2O$ as precursors and characterized by using a series method of XRD, FTIR, SEM-EDX and UV-visible diffuse reflectance. The catalytic activity of zeolite-supported PbO for removal of methylene blue was performed in the dark condition. The crystallite of zeolite-supported PbO having size of 23.2 nm was observed, but SEM-EDX measurement indicate the presences of zeolite-supported PbO and PbO having 2 to 8 μm and 0.5 to 2 μm in size, respectively, with PbO was spreaded over the surface of the zeolite. The PbO lowers the band gap energy (E_g) of the zeolite from 3.21 to 3.01 eV, allowing the catalysts works under either visible and UV light. The catalysts absorbs methylene blue following Freundlich isotherm absorption.

Keywords: Band gap, Photocatalysts, Photodegradation, Zeolite-supported PbO.

INTRODUCTION

The development of the textile industry has had a positive impact by reducing unemployment and the negative impact on the environment due to the waste produced which may reduce the aesthetic value of the waters as well as block the sunlight through the waters that can disturb the process of photosynthesis in the waters [1]. One of the dyes used in textile colouring is methylene blue which can cause cyanosis and skin irritation [2].

At the present time, environmental pollution caused by dyes has been so alarming that serious handling is needed to solve the problem. Several methods have been developed such as adsorption method using activated carbon, coagulation, sedimentation and active sludge. Conventional wastewater treatment is relatively easy in the process and does not require a high cost, but unfortunately the treatment is less than ideal. Waste treatment by coagulation method and sedimentation generate new coagulant that cannot be reused. In the adsorption method, the adsorbed dyes are accumulated in the adsorbent surface resulting in new problems to be addressed. Whereas in the used of active sludge method, some dyes indicate a biologically degradable resistant property [3-5]. Therefore, new alternatives in the effluent treatment of textile industry effectively and efficiently are needed.

One of the alternative methods of dyes treatment that has been developed at this time is photodegradation method by using photocatalyst semiconductors and ultraviolet light [6,7]. The photocatalytic process needs to be further developed because unlike conventional waste treatment which only moves pollutants from one place to another but is able to convert pollutants into simple and environmentally friendly compounds [6,8].

Among the various kinds of metal oxide semiconductors, titanium dioxide is one of the oxide semiconductors that have been studied extensively as a photocatalyst. Although TiO_2 is more commonly used as a photocatalyst, lead oxide (PbO) may also be used as a light-stable semiconductor photocatalyst so as to degrade the organic pollutants [9].

Band gap energy and electron-hole pair combination influenced by the particle size of the semiconductor material or the photocatalyst determine the activity of photocatalysis. Therefore many attempts are made to prepare photocatalysts with better particle size distribution. Many researchers dispersed semiconductor nanoparticles in solid-stable support materials such as silica, activated charcoal, clays and zeolites. Zeolite is one of good supports for dispersing PbO semiconductors because zeolites have large surface area and pore volume and uniformity of channel size [10]. Lead(II) oxide indicates high selectivity of photodegradation for methylene blue (MB) [11].

Based on this background, we report the preparation and characterization of Indonesian natural zeolite-supported PbO.

EXPERIMENTAL

Indonesian natural zeolite (moredenite type), $Pb(CH_3COO)_2{\cdot}3H_2O$ (Merck) and methylene blue (Sigma-Aldrich) were used as received without any further purification.

Prior to used, a mordenite type zeolite from Gunung Kidul, Indonesia, was physically activated in order to remove unwanted elements and evaporate water trapped in the pores of the zeolite structure. The process included sieving to obtain zeolites powder with the size of 100 to 200 mesh. The zeolite is then dispersed into aquades with a ratio of 1: 3 and stirred for 2 h at 90 °C. The remaining water was decanted and the remaining solid was dried at 120 °C in the oven and followed by calcination in the muffle furnace at 300 °C for 2 h.

The zeolite was further chemically activated by dispersing the zeolite in a mixture of aquademine and 1 M NaCl solution in a ratio of 1:4, stirring for 2 h and drying at 120 °C. Furthermore, the zeolite was calcined in a muffle furnace at 300 °C for 3 h.

Zeolite-supported PbO was prepared by mixing lead acetate solution with activated zeolite, heating at 50 °C and stirring for 2 h. This process allowed the Pb^{2+} ions entering the cavity or the of zeolite pores and bonding with the zeolite. Solution of 10 mL 0.1 M NaOH is added to the solid material, which then stirred for 1 h, allowing a hydrolysis reaction was undertaken producing a reactive species that is the reactive zeolite-supported $Pb(OH_4)^{2-}$. The zeolite-supported hydroxide species was then calcined at 400 °C to obtain zeolite-supported PbO catalysts.

The catalysts were then characterized using infrared spectrometry, powder X-ray diffraction (XRD Rigaku Multiflex), scanning electron microscopy (SEM Jeol JCM-6000), EDX and UV-visible spectroscopy (UV-2450PC Pharmaspec Spectrophotometer) methods.

The adsorption behaviour of zeolite-supported PbO catalysts was performed in the dark, in which 10 mL of methylene blue solutions with different initial concentrations were added with 0.1 g of zeolite-supported PbO powders and then stirred for 24 h. The methylene blue concentration in the suspensions before and after the adsorption were analyzed to determine the amount of methylene blue adsorbed by the catalyst.

RESULTS AND DISCUSSION

Infrared spectroscopy method has been used to observe the presence of functional groups in natural zeolite, activated zeolite and zeolite-supported PbO. The IR spectra are presented in Fig. 1. The vibration at 3465.19 cm^{-1} indicates the functional group -OH of the water molecule. The Pb-O vibration is indicated by a sharp line at 501.80 cm^{-1} and a weak line 578.64 cm^{-1}.

The selected vibrations of natural zeolite samples, activated zeolites and zeolite-supported PbO are listed in Table-1. In general, the natural zeolite, the activated zeolite and the zeolite-supported PbO indicate similar vibations, except vibrations observed at 501.49 and 578.64 cm^{-1} representing PbO. This is in agreement with the result of Borhade *et al.* [11,12].

TABLE-1
SELECTED VIBRATIONS OF NATURAL ZEOLITE SAMPLES, ACTIVATED ZEOLITES AND ZEOLITE-SUPPORTED PbO

Frequencies (cm^{-1})			Type of bonds
Natural zeolite	Activated zeolite	Zeolite-supported PbO	
–	–	501.49, 578.64	Pb–O stretching
794.26	787.00	787.00	O–Si–O
1092.77	1092.77	1092.77	Si–O–Si
2368.59	2337.72	2368.49	Si–H–Si
3465.19	3465.19	3465.19	OH–stretching

The powder XRD patterns of zeolite, activated zeolite and zeolite-supported PbO were collected at 2θ from 20° to 80°, step size 0.02° per second, using XRD Rigaku MiniFlex, CuK_α 1,5406 Å, 40 kW and 15 mA. The powder XRD patterns are depicted in Fig. 2. The powder XRD pattern of the natural zeolite indicates that the material is poorly crystalline (Fig. 2a). However few low-wide peaks at 2θ = 26.14° and 36.1° may be reffered to JCPDS (Joint Comitte for Powder Diffraction Standard) No. 6-239 of mordenite zeolite. Another very low and broad peaks belong to unrecognized species are also observed.

The unrecognized species are not observed in the XRD patterns of activated zeolite (Fig. 2b) and zeolite-supported PbO (Fig. 2c). It is belief that the unrecognized species were soluble in HCl and were removed during the activation process. The XRD patterns of the crystalline activated zeolite and the zeolite-supported PbO are consisted strong peaks at 2θ = 21.70°; 26.63°; 28.00°; 35.68°; 56.38°; 64.12° and 68.81° and 21.65°; 23.87°; 27.82°; 35.69°; 56.41°; 64.08° and 68.83°, repectively, indicating the presence of mordenite zeolite.

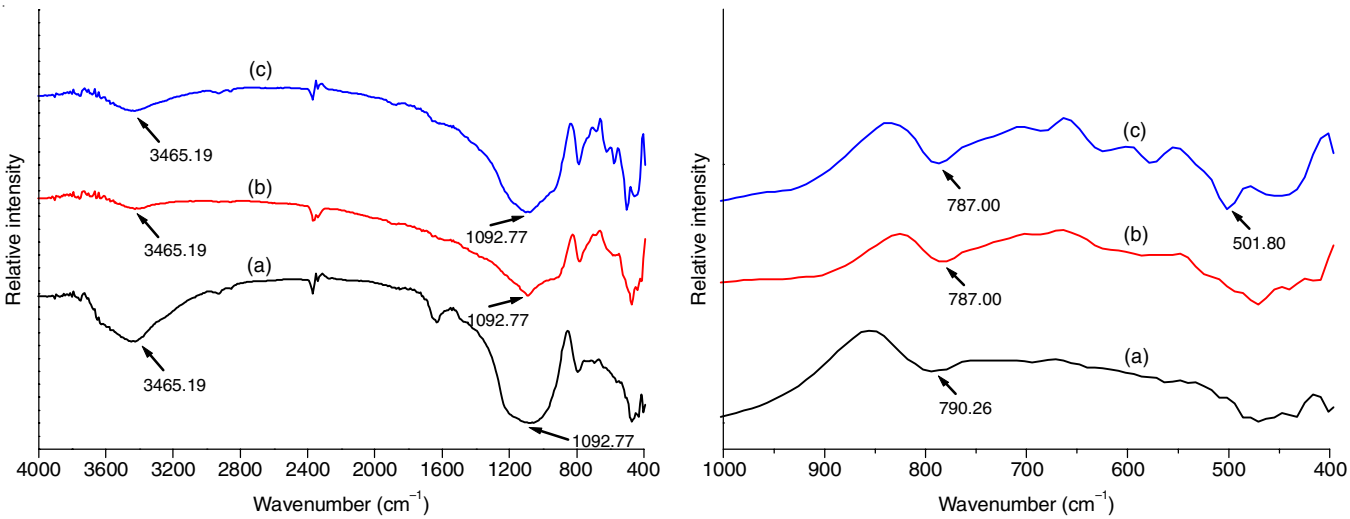

Fig. 1. IR spectra of zeolite (a), activated zeolite (b) and zeolite-supported PbO (c)

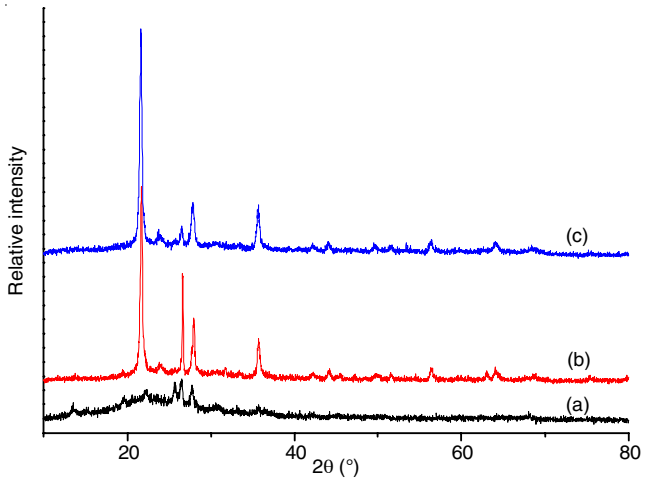

Fig. 2. Powder XRD pattern of zeolite (a), activated zeolite (b) and zeolite-supported PbO (c)

The presence of PbO over the zeolite supported are undefined, since the amount of PbO is very small resulting a very low XRD line compare to the support material.

The crystallite size of the natural zeolite, the activated zeolite and zeolite-supported PbO is determined by using the Scherrer equation. The average crystallite size of the materials is 25 nm (Table-2).

TABLE-2
CRYSTALLITE SIZE OF THE NATURAL ZEOLITE, THE ACTIVATED ZEOLITE AND ZEOLITE-SUPPORTED PbO

Material	Crystallite size (nm)
Natural Zeolite	32.50
Activated Zeolite	25.02
Zeolit-supported PbO	23.20

A combination of SEM-EDX method has been used to analyze the surface morphology, particle size and elemental composition of the zeolite-supported PbO material. The micrograph of the zeolite-supported PbO is shown in Fig. 3. The material indicates rough surfaced and irregular shaped clumps suspected to be zeolite support with a size of about 2-8 micrometers. EDX analysis confirms the presence of PbO (Fig. 4) as small particles (0.5 to 2 µm) randomly distributed over the zeolite surface (Fig. 3).

The activated zeolite and zeolite-supported PbO materials were studied using the UV-visible 1700 spectrophotometer (Ultraviolet visible diffuse reflectance) to determine the optimum absorbances and the band gap energies. Prior to the measurements, the catalysts were dissolved in a mixture of Triton X and acetylacetonate to form pastes, which were then layered on the preparatory glass. The glass were then dried in a furnace at 450 °C for 2 h to evaporate the remaining solvent. Measurements were carried out at wavelengths of 200-800 nm (Fig. 5). Each sample absorbed energy at certain wavelength(s). The activated zeolite indicates a maximum absorbance at wavelength of 281 nm which is a UV light region. For zeolite-supported PbO the maximum absorbance is observed at wavelength 467 nm which is at visible region. This indicate that the introduction of PbO on zeolite shifts the maximum absorbance from UV to visible regions.

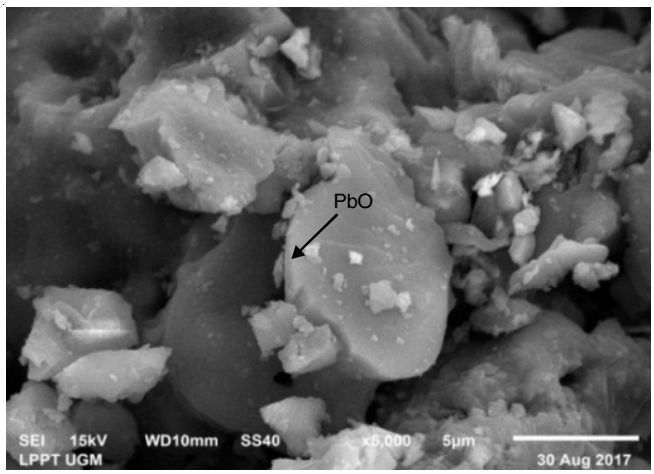

Fig. 3. Electron micrograph of the zeolite-supported PbO

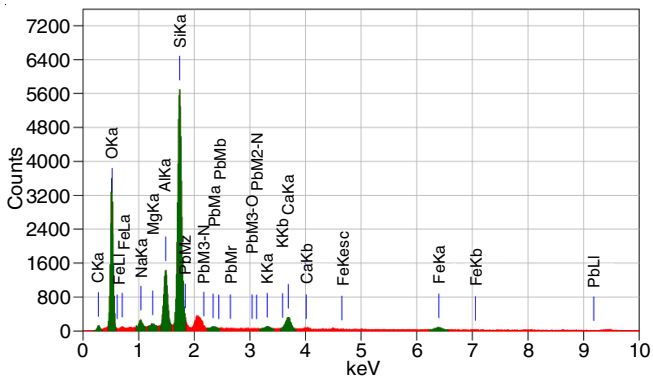

Fig. 4. EDX spectra of the zeolite-supported PbO

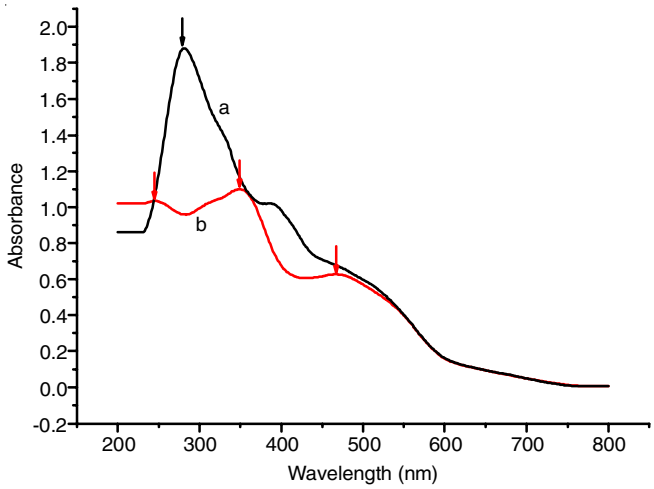

Fig. 5. Absorbance of activated zeolite (a) and zeolite-supported PbO (b)

The Kubelka-Munk equation was used to calculate the band gap energy (E_g) of catalysts. Figs. 6 and 7 depicts plots to obtaining band gap energies of activated zeolite and zeolite-supported PbO. The band gap energy of activated zeolite and zeolite-supported PbO are 3.21 eV and 3.01 eV, respectively. The decreasing band gap from 3.21 to 3.01 eV (0.20 eV) is definetly caused by the addition of PbO to the zeolite. This is in accordance with the former findings concluding that the band gap energy of PbO is 2.9 eV [13,14].

Determination of catalyst adsorption pattern was performed using Langmuir and Frundlich equations. The Langmuir isotherm pattern was undertaken by correlating the methylene

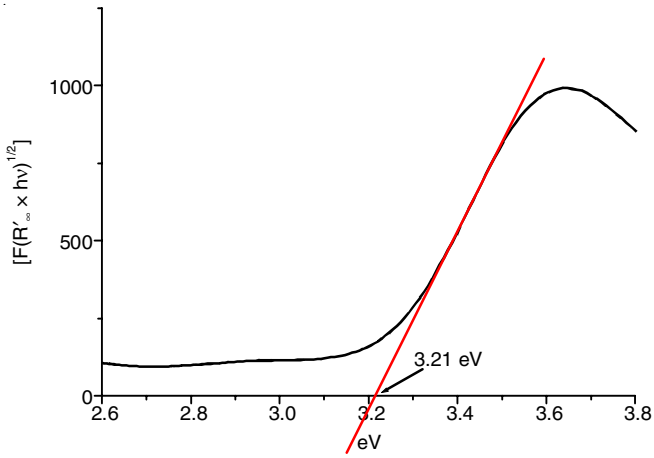

Fig. 6. Band gap enegy of the activated zeolite

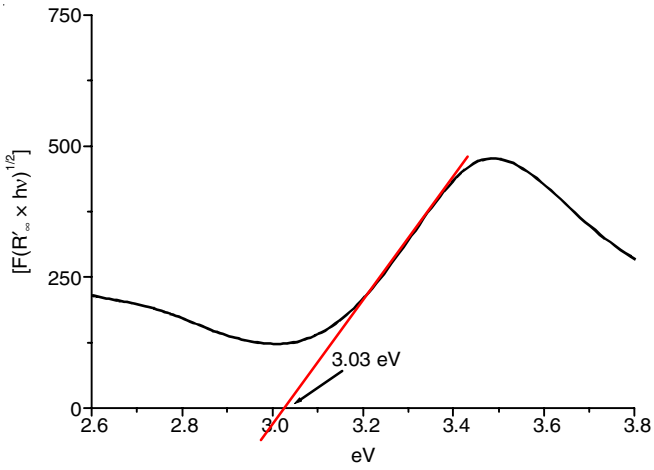

Fig. 7. Band gap enegy of zeolite-supported PbO

blue concentration adsorbed on every 1 g of catalyst (c/m) with the methylene blue concentration after 24 h (c). The calculation of the adsorption capacity value (b) on the Langmuir isotherm was undertaken using equation as follows:

$$\frac{c}{m} = \frac{c}{b} + \frac{1}{K_L b}$$

Freundlich isotherm pattern was determined by plotting the log value of the amount of methylene blue adsorbed on every 1 g of catalyst (log x/m) with the log of methylene blue concentration after 24 h (log c). The calculation of the adsorption capacity (k) of the Freundlich isotherm was undertaken using equation as follows:

$$\log \frac{x}{m} = \log k + \frac{1}{n} \log c$$

The equation of Langmuir and Freundlich isotherms are resumed in Table-3.

TABLE-3
EQUATIONS OF LANGMUIR AND FREUNDLICH ISOTHERM PATTERNS OF THE ZEOLITE-SUPPORTED PbO

Catalysts	Langmuir	Freundlich
Zeolite-supported PbO	y = 250.6 x + 0.0007 R^2 = 0.9009	y = 173420x – 5.6249 R^2 = 0.9243

The R^2 values of the Freundlich adsorption isotherm pattern are higher than that of the Langmuir. Thus, it is concluded that the adsorption on methylene blue by zeolite-supported PbO follows Freundlich isotherm pattern.

Conclusion

The zeolite-supported PbO has been prepared using Indonesian natural zeolite and lead acetate as precursors. The crystallite size of zeolite-supported PbO is 23.2 nm. SEM-EDX measurement indicates the zeolite-supported PbO and PbO having 2 to 8 μm and 0.5 to 2 μm in size, respectively. The PbO lowers the band gap energy (E_g) of the zeolite as high as 0.2 eV. This allows the catalysts working either under visible and UV light.

REFERENCES

1. C.D. Raman and S. Kanmani, *J. Environ. Manage.*, **177**, 341 (2016); https://doi.org/10.1016/j.jenvman.2016.04.034.
2. P.A. Kouides, C.N. Abboud and V.F. Fairbanks, *Br. J. Haematol.*, **94**, 73 (1996); https://doi.org/10.1046/j.1365-2141.1996.d01-1766.x.
3. B.H. Hameed, A.T.M. Din and A.L. Ahmad, *J. Hazard. Mater.*, **141**, 819 (2007); https://doi.org/10.1016/j.jhazmat.2006.07.049.
4. B.H. Hameed, A.L. Ahmad and K.N.A. Latiff, *Dyes Pigments*, **75**, 143 (2007); https://doi.org/10.1016/j.dyepig.2006.05.039.
5. M.A. Rahman, S.M.R. Amin and M.S. Alam, *Dhaka Univ. J. Sci.*, **60**, 185 (2012); https://doi.org/10.3329/dujs.v60i2.11491.
6. M.R.D. Khaki, M.S. Shafeeyan, A.A.A. Raman and W.M.A.W. Daud, *J. Environ. Manage.*, **198**, 78 (2017); https://doi.org/10.1016/j.jenvman.2017.04.099.
7. A.K. Prodjosantoso, T. Rahmawati and C. Kusumawardani, *Res. J. Chem. Environ.*, **21**, 12 (2017).
8. U.I. Gaya and A.H. Abdullah, *J. Photochem. Photobiol. Photochem. Rev.*, **9**, 1 (2008); https://doi.org/10.1016/j.jphotochemrev.2007.12.003.
9. D.S. Bhachu, S. Sathasivam, C.J. Carmalt and I.P. Parkin, *Langmuir*, **30**, 624 (2014); https://doi.org/10.1021/la4038777.
10. M. Babaahamdi-Milani and A. Nezamzadeh-Ejhieh, *J. Hazard. Mater.*, **318**, 291 (2016); https://doi.org/10.1016/j.jhazmat.2016.07.012.
11. A.V. Borhade, D.R. Tope and B.K. Uphade, *E-J. Chem.*, **9**, 705 (2012); https://doi.org/10.1155/2012/362680.
12. A.V. Borhade, B.K. Uphade and D.R. Tope, *J. Chem. Sci.*, **125**, 583 (2013); https://doi.org/10.1007/s12039-013-0396-8.
13. E.C. Ekuma, E.V. Esabunor and E. Osarolube, *Optoelectron. Adv. Mater. Rapid Commun.*, **5**, 960 (2011).
14. D.O. Scanlon, A.B. Kehoe, G.W. Watson, M.O. Jones, W.I.F. David, D.J. Payne, R.G. Egdell, P.P. Edwards and A. Walsh, *Phys. Rev. Lett.*, **107**, 246402 (2011); https://doi.org/10.1103/PhysRevLett.107.246402.